FEASIBILITY OF AN ON-BOARD MICRO-ORC SYSTEM FOR SMALL SATELLITES

Fiona Leverone[1*], Matteo Pini[1], Angelo Cervone[1], Eberhard Gill[1]

[1] Delft University of Technology, Aerospace Engineering Faculty,
2629 HS, Delft, The Netherlands
F.K.Leverone@tudelft.nl

* Corresponding Author

ABSTRACT

Small satellites are receiving increased recognition in the space domain due to their reduced associated launch costs and their shorter lead time when compared to larger satellites. However, this advantage is often at the expense of mission capabilities, such as available electrical power and propulsion. A possible solution is to change from the conventional solar photovoltaic and battery configuration to a micro-Organic Rankine Cycle (ORC) and thermal energy storage system that uses the waste energy from a solar thermal propulsion system. This unique approach has the potential to offer higher system efficiency and power density. However, limited literature is available on micro-ORC systems, which are capable of producing a few hundred Watts of electrical power, especially for small satellites. A feasibility study of these systems and a fluid selection study were conducted. This was done by using a multi-objective genetic algorithm to optimise an on-board micro-ORC system for various working fluids such as Toluene (C7H8), Hexamethyldisiloxane (MM), and Octamethylcyclotetrasiloxane (D4). The two objective functions were to minimise the total volume and maximise the thermal energy storage capacity. This paper describes the proposed system layout and model of the integrated micro-ORC system. The specific objectives of this study are: i) the working fluid selection, and ii) the optimisation of the proposed system incorporating the design of the thermodynamic cycle and the sizing of the turbine and heat exchangers. Results show that the design of the micro-ORC system is dependent on the mission designer requirements, and various design configurations are provided from the Pareto frontier. It was also found that when the surface wall temperature of the evaporator is near the thermal stability limit of the working fluid, the evaporator operates in the dispersed film boiling regime which reduces the heat transfer coefficient. Additional challenges include high micro-turbine rotational speeds, large thermal cycling, small blade heights, and large condensers. Finally, the storage configuration of the concentrator was identified as crucial for the feasibility of the system on-board small satellites.

1. INTRODUCTION

The increase of electrical power consumption required by small satellites promotes the need for on-board power sources that have high energy and power densities. This increase is especially important for future planned interplanetary missions proposed by NASA. Future missions are estimated to need power densities in the range of 150 and 250 W/kg (Surampudi et al., 2017b) and specific energies greater than 250 Wh/kg (Surampudi et al., 2017a). Conventionally, small satellite power systems consist of photovoltaic technologies which have a specific power from around 20 W/kg to 100 W/kg (Antonio et al., 2019; Montgomery et al., 2019). Power systems can also include an on-board energy storage device, with advanced lithium-polymer or -ion batteries being the most commonly used. These batteries have specific energies between 150 to 250 Wh/kg. These systems may not be suitable for future missions, and therefore, alternative power systems should be investigated. A possible alternative system that has the potential to offer high power densities is the micro-Organic Rankine Cycle (ORC) system (Leverone et al., 2017). Here micro refers to power levels of 100 to 500 W.

To further extend the capabilities of a small satellite and to achieve missions, such as interplanetary

missions, a propulsion system is also required. Solar thermal propulsion (STP) has been identified as a possible cost-effective solution (Leverone et al., 2019). STP is a system that generates thrust by using concentrated solar radiation to heat a propellant to high temperatures of more than 1500 K, to increase the performance over conventional propulsion systems. Coupling an STP system with a micro-ORC system, as shown in Figure 1a, could improve the system efficiency to develop small high-performance satellites by using the wasted energy from the STP system to co-generate electrical power and propulsion (Leverone et al., 2017). The waste heat could also be used for on-board thermal control.

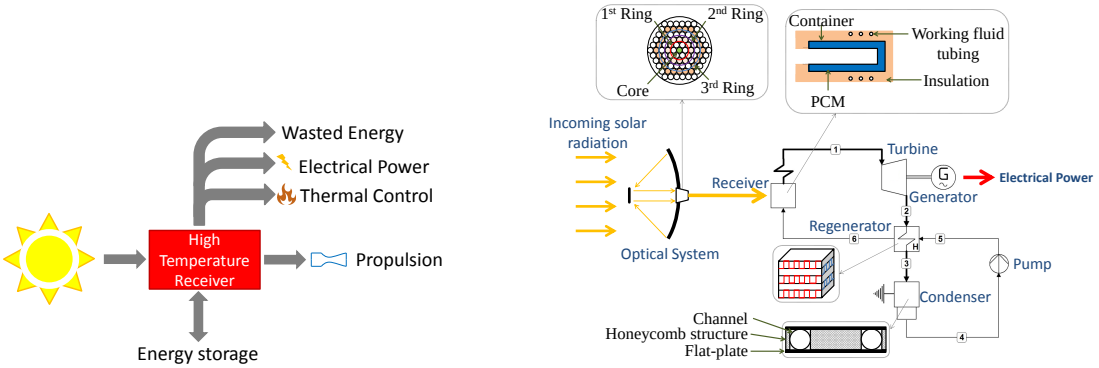

Figure 1: Sysytem schematics: (a) complete integrated solar thermal system and (b) the mirco-ORC system.

The idea of using an ORC for power generation in space dates back to the 1960s (Angelino et al., 1991; Schubert, 2012). Large scale ORC systems, with power capacities on the order of 1 to 30 kW, were proposed to power the International Space Station. ORC systems are attractive for space applications as they can have a higher resistance to degradation in the space environment compared to photovoltaic systems (Angelino et al., 1991; Schubert, 2012). It has also been noted that a micro-scale Rankine cycle has potentially better thermal efficiency and higher power density versus Brayton cycles. This improvement is due to the poor compression efficiency of the micro-Brayton cycle that reduces the design space to pressure ratios less than 5. Rankine cycles can lead to lighter designs which are critical for small satellites. Drawbacks of a micro-ORC system are lack of space heritage and reduction in reliability due to the ORC system having more moving parts than the PV-battery system, as well as potential transient inertial effects during start-up and shutdown, leakages, supersonic flow in the stator, and high rotational speeds (Angelino and Invernizzi, 1993; Harinck et al., 2010; Uusitalo et al., 2014).

Research on micro-ORC systems, from a few Watts to 2 kW, has focused on solar thermal and waste energy power generation in portable electronic, miniature robotic, automobile, and remote off-grid applications (Fréchette et al., 2004; Roudy and Frechette, 2005; Orosz, 2009; Liamini et al., 2010). However, little is known on the topic of micro-ORC systems, especially for small satellite applications, and investigations have often neglected the sizing of the components such as the turbine and heat exchangers (Schubert, 2012). Therefore, an investigation into the feasibility of generating power from the wasted heat energy of a solar thermal propulsion system on-board a small satellite is required. This study focuses on developing a micro-ORC system that meets the manufacturing and operational constraints while still conforming to the performance requirements. The feasibility is determined based on a multi-objective optimisation analysis using a genetic algorithm. The two objective functions are the total system volume and the thermal energy storage capacity.

2. SYSTEM DESCRIPTION

A schematic of the proposed micro-ORC system, excluding the propulsion system is shown in Figure 1b. The major challenge with integrating an ORC with an STP system for space applications is the conflicting operating temperatures. The STP requires propellant temperatures above 1500 K to achieve

high performance, whereas the ORC has a maximum operating temperature of approximately 600 K, depending on the working fluid and its corresponding thermal stability limit. Available literature reports the thermal stability limit for MM as 300 °C (Preißinger and Brüggemann, 2016) and for cyclic siloxanes (Colonna et al., 2006; Angelino and Invernizzi, 1993) and toluene as 400 °C (Trimm et al., 1990). No literature was found regarding the thermal stability of MDM, for this research, it is assumed as the lower limit of 300 °C.

Gilpin (2015), has identified silicon and boron as high-temperature phase change materials (PCM) that are near- and far-term solutions for STP receivers respectively. Therefore, silicon has been selected as the receiver material and heat source for this work. The receiver is assumed to be cylindrical and is made up of a silicon phase change material (PCM), a boron nitride container, and uses carbon bonded carbon fibre (CBCF) as the insulation material. The receiver also includes a rhenium coating for oxidation protection. The aperture diameter of the receiver is designed to accommodate all the optical fibres entering the receiver, which are part of the optical system. The receiver also acts as a latent heat storage device. Advantages of using a latent heat storage system are that it can operate at relatively constant temperatures and has high energy storage densities, both of which are attractive qualities for ORC systems and small satellites. The thermal energy stored is crucial to ensure continuous electrical power generation during eclipse periods, therefore not limiting the operations of the small satellite during orbit. Challenges include thermal stresses, radiation losses, and containment of the phase change material. The inclusion of a heat transfer loop between the high-temperature receiver and working fluid was discarded because it would decrease the efficiency of the system due to the addition of another pump as well as increase complexity and therefore reduce the reliability of the system. This work, therefore, investigates the possibility of directly embedding the working fluid tubing inside the receiver's insulation, such that the maximum temperature exposed to the working fluid tubing is 20 K less than the thermal stability limit of the fluid.

The optical system, which concentrates solar radiation onto a high-temperature receiver consists of a primary and secondary concentrator and fibre optic cables. A parabolic primary dish was chosen as it can achieve higher concentration ratios than both spherical mirrors and Fresnel lenses or mirrors, which suffer from spherical or chromatic aberration (Kreider, 1979). A non-concentrating flat plate secondary concentrator was selected due to simplicity and ease of manufacture over improving the performance. The main function of the flat plate concentrator is to increase the ease of optical fibre placement, reduce the length of the optical fibre required between the concentrator and the receiver, and make the design more compact (Henshall, 2006). Fibre optic cables have been included in the design instead of directly focusing solar radiation onto the receiver to reduce the pointing accuracy required and decouple the concentrator and receiver position. This is also a requirement from the propulsion side such that the concentrator position does not constrain the satellite manoeuvring direction. Additionally, they provide the system with the potential to reduce the overall mass by replacing a single large mirror with multiple smaller ones (Henshall, 2006). Disadvantages of the selected optical configuration include decreased end-to-end power efficiency, increased complexity and storage integration challenges.

The solar radiation collected by the receiver superheats the working fluid that is passed through the evaporator tubing coiled inside the insulation of the receiver. The condenser radiates heat to space to condense the working fluid. The condenser is made up of several circular channels, a honeycomb support structure, and two thin flat sheets of aluminium on the top and bottom that radiate to space. A regenerator is included before the condenser to improve the efficiency of the ORC system. It also reduces the heat transfer surface area of the receiver and condenser at the expense of increased complexity and mass as well as reduced reliability. The regenerator is assumed to be a cross-flow plate-fin heat exchanger with rectangular channels due to its compactness, lightweight, and ability to operate at high temperatures. A radial inflow turbine is coupled to a generator to provide on-board electrical power. The selection of this turbine was mainly due to its high power density and compactness, which are critical aspects for small satellite sub-systems.

3. MODEL DESCRIPTION

An investigation into the feasibility of a micro-ORC system in terms of volume and thermal energy storage (TES) discharge time has been conducted. Only simple superheated saturated configurations with regeneration are analysed. This was achieved by using a genetic algorithm (GA) based on the system architecture shown in Figure 1b. Genetic algorithms are common methods used in ORC optimization studies due to their robustness, however at the expense of higher computational time when compared to other methods such as the direct search and variable metric method. The optimization population size was set to 140 and the termination criteria was set as either a convergence criterion of 10^{-10} or a maximum number of generations of 300. These values were selected as a compromise between computational speed and accuracy. An initial mutation rate of 0.02 and a crossover probability of 0.7 were also used. The optimization has 14 design variables for each working fluid analysed. These variables are the maximum and minimum cycle pressure, the regenerator fin height, fin thickness, fin frequency, number of hot layers, and the length of both the hot and cold side of the regenerator, as well as the condenser diameter, number of concentrators, number of fibres, and receiver thickness, length, and insulation thickness. Optimization constraints and constants used are shown in Table 1 and are based on the satellite's mission constraints, manufacturing limitations, and flow conditions. When these constraints are exceeded the solution of the given population is disregarded.

Table 1: Optimization constraints and system model parameters.

Constraints		Comment	Model parameters		Comment
Rotor blade height:	$b > 0.2$ mm	Manufacturing limit	Stator inlet to outlet radius ratio:	$\frac{r_0}{r_1} = 1.3$	Flow condition
Regenerator thickness to height ratio:	$\frac{X_5}{X_4} < 1$	Manufacturing limit	Stator outlet to rotor inlet radius ratio:	$\frac{r_1}{r_2} = 1.02$	Flow condition
Regenerator thickness:	$X_5 \geq \frac{p}{\eta_{fin}\sigma_{fin}}$	Manufacturing limit	Rotor shroud outlet to inlet radius:	$\frac{r_{2,3}}{r_2} = 0.7$	Flow condition
Receiver length to evaporator length:	$\frac{L_{rec}}{L_{ev}} \geq 1$	Manufacturing limit	Rotor outlet hub to shroud radius ratio:	$\frac{r_{h,3}}{r_{s,3}} = 0.4$	Flow condition
Max. cycle pressure:	$X_2 \leq 0.95 p_{crit}$	Flow condition	Absolute flow angle, rotor inlet:	$\alpha_2 = 80°$	Flow condition
Min. to max. cycle pressure ratio:	$\frac{X_3}{X_2} < 1$	Flow condition	Relative flow angle, rotor exit:	$\beta_3 = 60°$	Flow condition
Relative rotor Mach Number:	$M_{2,rl} < 0.85$	Flow condition	Axial flow coefficient:	$\varphi = 0.3$	Flow condition
Relative flow velocity ratio:	$\frac{w_3}{w_2} > 1.5$	Flow condition	Spacecraft volume and mass:	$V_{sc} = 0.3976\,\mathrm{m}^3$, $M_{sc} = 215\,\mathrm{kg}$	Satellite mission
Regenerator pinch point temperature:	$\Delta T_{pp,rg} \leq 20$	Flow condition	Eclipse time:	$t_{eclipse} = 35,29$ minutes	Satellite mission
Max. evaporator wall temperature	$T_{wall} = T_{stability} - 20$	Flow condition	Turbine, pump and generator isentropic efficiency:	$\eta_t = 65\%$, $\eta_p = 50\%$, $\eta_g = 100\%$	Flow condition
Max. working fluid temperature	$T_{wf} = T_{sat} + 10$	Flow condition	Solar flux and Sun half-angle:	$S = 1350\,\mathrm{W/m}^2$, $\theta = 0.266°$	Satellite mission
			Optical fibre efficiency:	$\eta_f = 83.8\%$	Manufacturing limit
			Fibre mass per length:	$L = 9.95$ g/m	Manufacturing limit
			Shadow factor:	$b = 0.02$	Manufacturing limit

For this study, the optimisation minimises the objective function, $F(x)$, in Equation 1, which is defined using the weighted sum approach and parabolic penalty method. The terms in Equation 1 are squared to reduce the risk of a non-convex solution where optimal points cannot be found. The penalty factor ($\Omega = \sum P(x)$) is added to converge infeasible simulations to feasible solutions so that the infeasible results are discarded in the successive iteration, but the search domain is not limited. A penalty is given if the fluid velocity in the heat exchangers is outside the boundary defined by the heat exchangers for liquid, gas, or two-phase flow (Caputo et al., 2011). Penalties are also given if the flow falls outside the ranges given by the correlations used for the condenser and evaporator. The penalty factor is defined as the summation of all these penalties which are individually calculated as, $P_i = \chi/\chi_{\max}$, if $\chi > \chi_{max}$ or $P_i = \chi_{\min}/\chi$, if $\chi < \chi_{\min}$, where χ is an arbitrary parameter that represents the parameter that is out of the feasible boundary.

$$F(x) = w_1\{\mu_1(x)\}^2 + w_2\{\mu_2(x)\}^2 + \{\Omega\}^2 \tag{1}$$

where w_1 and w_2 are the weights and are constrained to $w_1 + w_2 = 1$ and $0 \leq w_i \leq 1, i = 1, 2$, μ_1 is the first design objective to minimise volume ($\mu_1 = V_{tot}/V_{sc}$) and μ_2 is the second design objective to maximise the discharge time ($\mu_2 = t_{eclipse}/t_{dis}$). The total volume of the ORC system, V_{tot}, is the summation of the volume of the evaporator, regenerator, condenser, pump, plumbing, and turbine. An additional margin of 20% has been included to account for miscellaneous components such as support structures, interfaces, and control hardware. The total volume of the satellite is denoted by V_{sc} and is determined based on the allowable payload volume inside the standard Evolved Expendable Launch Vehicles (EELV) Secondary Payload Adapter (ESPA). The eclipse time that the satellite experiences is denoted as $t_{eclipse}$ and the steady-state discharge time of the thermal energy storage system is t_{dis}.

The optimisation methodology involves first thermodynamically analysing the ORC system excluding pressure losses. When the ORC system meets the constraints shown in Table 1, the heat exchangers sizing are evaluated, and if feasible, the ORC is then re-evaluated incorporating the pressure losses. Next, the concentrator and the receiver are analysed. This process is carried out until the termination criterion is met.

3.1 System Model

The steady-state thermodynamic analysis of the ORC system has been carried out using an in-house Matlab code based on the work of Bahamonde et al. (2017). Fluid thermophysical properties are determined by integrating the code with the software library Fluidprop (Colonna and Van der Stelt, 2004). Each heat exchanger (HX) has been discretised to evaluate the one-dimensional local heat transfer coefficient and pressure drop in the single phase and two-phase flow regions to determine its size. The plate-fin rating model and ϵ-NTU method discussed in Shah, Ramesh K and Sekulic (2003) are used in this analysis for the regenerator. The heat transfer coefficient correlations used for the two-phase condensing flow region are defined by Kim and Mudawar (2013a). The area of the radiator is determined based on the heat-pipe analysis described by Gilmore (2002, Chapter 6). The single phase Nusselt number correlations, two-phase pressure gradients, radiation heat transfer coefficient are provided in Table 2. The thermal stability limit of the working fluid could result in low/high quality critical heat flux (CHF) regimes. This can considerably reduce the heat transfer coefficient. The CHF quality is determined using the method proposed by Shah (2017). If the CHF quality is low, boiling is split into Inverted Annular Flow Boiling (IAFB) and Dispersed Flow Film Boiling (DFFB) regimes. If the flow is in the saturation two-phase boiling regime, the heat transfer coefficient is modelled based on the universal approach described by Kim and Mudawar (2013b,c). Dryout at high qualities will result in DFFB being present after saturated boiling flow. The selection of empirical correlations used for boiling heat transfer coefficients is provided in Section 4.

Table 2: Correlations used in the heat exchangers.

Equations	
Laminar developing flow: Rectangular channel	**Accelerational pressure drop:**
$f_{app} = \frac{1}{\mathrm{Re}}\left[3.44\left(x^*\right)^{-0.5} + \frac{K(\infty)/(4x^*)+f\mathrm{Re}-3.44\left(x^*\right)^{-0.5}}{1+C\left(x^*\right)^{-2}}\right]$	$-\left(\frac{dp}{dz}\right)_A = G^2\frac{d}{dz}\left[\frac{x^2}{\alpha\rho_g} + \frac{(1-x)^2}{(1-\alpha)\rho_f}\right]$
$\mathrm{Nu} = \left[0.277 - 0.152e^{\left(-38.6x^*\right)}\right]^{-1}$	$\alpha = \left[1 + \left(\frac{1-x}{x}\right)\left(\frac{\rho_g}{\rho_f}\right)^{2/3}\right]^{-1}$
Laminar fully developed flow: Rectangular channel	**Frictional pressure drop:**
$f = \frac{24}{\mathrm{Re}}\left(1 - 1.35553\beta + 1.9437\beta^2 - 1.7012\beta^3 + 0.9564\beta^4 - 0.2537\beta^5\right)$	$\left(\frac{dp}{dz}\right)_F = \left(\frac{dp}{dz}\right)_f\phi_f^2 = \frac{2fG^2(1-x)^2}{D_{hyd}\rho_f}\phi_f^2$, Two phase
$\mathrm{Nu} = 8.235\left(1 - 2.0421\beta + 3.0853\beta^2 - 2.4765\beta^3 + 1.0578\beta^4 - 0.1861\beta^5\right)$	$\left(\frac{dp}{dz}\right)_F = \frac{2fG^2}{D_{hyd}\rho}$, Single phase
Laminar developing flow: Circular channel	**Radiation heat transfer coefficient:**
$f = \frac{16}{\mathrm{Re}}$	$h_{rad} = \left(\frac{1}{\epsilon_w} + \frac{1}{\epsilon\sqrt{1-\alpha}} - 1\right)^{-1}$, for IAFB* and Saturated flow
$\mathrm{Nu} = 4.364$	$h_{rad} = \left(R_w + R_d + \frac{R_w R_d}{R_v}\right)^{-1} + \left(R_w + R_v + \frac{R_w R_v}{R_d}\right)^{-1}$ for DFFB flow
Turbulent fully developed flow: Rectangular channel	
$f = \frac{1}{4}\frac{1}{(0.790\ln(\mathrm{Re})-1.64)^2}$	
Turbulent fully developed flow: Circular channel	
$f = \frac{0.079}{\mathrm{Re}^{0.25}}, 2000 \le \mathrm{Re} < 20000, f = \frac{0.046}{\mathrm{Re}^{0.2}}, \mathrm{Re} \ge 20000$	$\mathrm{Nu} = \frac{\frac{f}{2}(\mathrm{Re}-1000)\,\mathrm{Pr}}{1+12.7\left(\sqrt{\frac{f}{2}}\left(\mathrm{Pr}^{\frac{2}{3}}-1\right)\right)}$

*void fraction is taken as zero for the IAFB region for simplicity.

The radial inflow turbine geometry was analysed based on first principles based on the model proposed in Bahamonde et al. (2017). For this model, it is assumed that the change in kinetic energy is negligible between the turbine inlet and outlet, that the flow in the stator is isentropic, and both the flow angle and blade angle are equal at the blade exit. The turbine mass and volume are estimated assuming the turbine is a solid disk with a diameter equivalent to the stator and the length equal to the axial length of the turbine.

A survey was conducted on available micro-pumps and generators suitable for a 200 W micro-ORC. The result of the micro-pump study shows that for low mass flow rates, the volume of the micro-pump remained the same for different differential pressure. For higher mass flow rates the volume increases. For simplicity the pump volume and mass are equal to the maximum values found from the survey rounded up to 0.001 m^3 and 1.5 kg respectively to be more conservative. Linear relationships were derived to relate the mass ($M_{gen} = 0.0018W_{net} + 2.718$) and volume ($V_{gen} = 2\times10^{-6}W_{net} + 7\times10^{-5}$) of the generator to the net power output W_{net}.

Determining the stowed volume is difficult without a full design of the concentrating and deployment

system. For this analysis, the stowed volume of the concentrator is assumed to be a percentage of a rigid design with the same geometry. The volume that the rigid system occupies is taken as cylindrical with the diameter equal to the primary concentrator and the height equal to the distance between the two concentrators plus the thickness of the secondary concentrator. The stowed volume is therefore dependant on the type of concentrating system: 1) fixed-rigid (100%), 2) deployable-rigid (25%) or 3) inflatable (1%) (Olla, 2009). For this study the concentrator and support areal densities are assumed to be 1 and 1.5 kg/m^2 respectively (Henshall, 2006; Gilpin, 2015) and an inflatable storage volume configuration was assumed.

A one-dimensional steady-state radial analysis using a temperature-dependent thermal conductivity and shell thickness method (Bergman et al., 2011) is used to determine the radiation losses through the insulation as well as the position of the working fluid tubing. The radiation loss though the aperture and the absorption losses of the receiver are also included. From this an estimated discharge time, $t_{dis} = E_{stored} / \dot{Q}_{out}$, based on the thermal energy storage, can be computed if the power available is greater than the losses. The receiver is assumed to act as a lumped-capacity thermal mass with no temperature distribution; this is only valid for low Biot numbers (<< 1). Therefore this results in a preliminary analysis that requires future in-depth analysis to more accurately determine the coupled convective heat transfer between the PCM, insulation, and the working fluid, as well as the solar flux input. Furthermore, analytical and experimental investigations into the thermal cycling and expansion of the PCM and long exposure between the PCM and its container are required. The expansion of silicon during freezing was not considered in this study. However, it has been found that by reducing the fill factor of the PCM by 80% the container damage due to the expansion can be mitigated (Gilpin, 2015). The volume and mass of the receiver are found based on its described geometry 1b, assuming that the length of the inner cavity of the receiver is 80% of the total length of the phase change material.

4. RESULTS AND DISCUSSION

To the authors knowledge, no ORC optimization study has included the effects of boiling flow in the IAFB and DFFB regimes. Figures 2a and 2b show existing IAFB empirical correlations compared with experimental data to identify which empirical correlations are suitable for this study. The empirical correlations are provided in (Hewitt et al., 2013). The results indicate that the correlations that perform the closest with the experimental data are the models proposed by Breen and Westwater, and Bromley based on either using the vapour or vapour film temperature for the IAFB regime. The closest performing DFFB correlations are the Bishop, Tong and Slaughterbeck correlations. The experimental IAFB data for R134a and water is obtained from Nakla et al. (2011), and the water DFFB experimental data is provided by Nguyen and Moon (2015) and Becker et al. (1983). The predicted heat transfer coefficients from the Andersen correlation exceeds the value of 1.5 kW/mK and therefore, do not appear in Figure 2a. Care must be taken for the DFFB regime as limited data points were available.

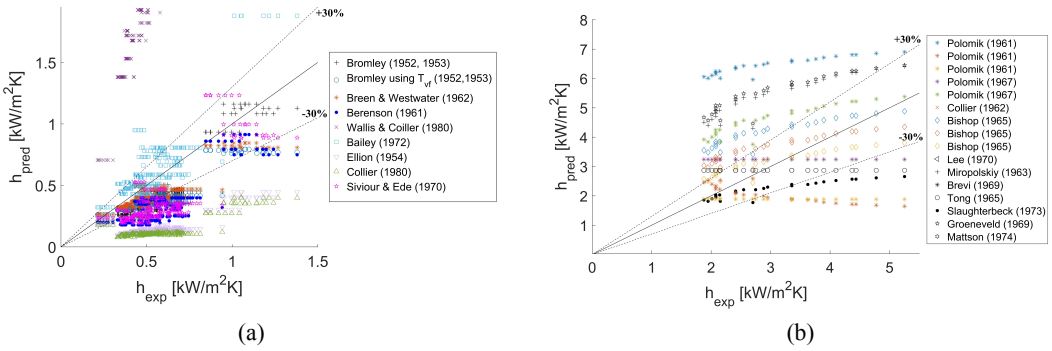

(a) (b)

Figure 2: Predicted versus experimental heat transfer coefficients: (a) IAFB and (b) DFFB regieme.

A sensitivity analysis was conducted on the two-phase boiling heat transfer coefficient to minimise the uncertainty, due to a lack of experimental validation of the correlations and working fluid considered in this study. The results in Table 3, where constant heat transfer coefficients were analysed, indicate as expected an increase in evaporator length and volume with decreasing heat transfer coefficient. However, the ORC volume and thermal efficiency are not significantly affected. The Bromley and the Bishop correlations were selected for use in the optimization study as they provided the most comparable values with the experimental data, Figure 2. These correlations also provided average results when compared to the other correlations during a one-at-a-time sensitivity analysis, Figure 3. This sensitivity analysis was conducted on various operating pressures (1, **10**, and 20 bar), tube diameters (1, **2**, 3, and 6 mm), surface wall temperatures (500, 550, and **650** K) and mass flow rates (1, 5, and **10** g/s), that are expected to occur during the optimization study, with the baseline parameters indicated in bold. The maximum working fluid (bulk) temperature was constrained to 10 K above its saturation temperature. It was found that the diameter has the largest influence on the DFFB heat transfer coefficient and that most IAFB correlations are not affected by the mass flow rate. During this sensitivity analysis, the radiation heat transfer coefficient accounted for a maximum of 6% of the total heat transfer coefficient for both the Bromley and the Bishop correlations, assuming a wall and liquid emissivity of 0.95 and 0.6 respectively.

Table 3: Constant heat transfer coefficient sensitivity analysis.

Heat Transfer Coefficient [W/m^{2}K]	Tube Length [*m*]	Evaporator Volume (x10^{-6}) [m^3]	ORC Volume [m^3]	ORC Thermal Efficiency [%]
100	7.056	67.90	0.078	12.71
500	1.752	16.90	0.078	12.74
1000	1.086	10.40	0.078	12.75
5000	0.553	5.32	0.078	12.75
10000	0.486	4.67	0.078	12.75
50000	0.432	4.16	0.078	12.75

Table 4: Results of minimum volume solutions found on the Pareto front (Figure 4a).

	Rotor blade height [mm]	Rotor rotational speed [krpm]	Thermal efficiency [%]	Toltal specific power [W/kg]	Shared specific power [W/kg]
Toluene	0.27	762	12.64	3.57	8.66
D4	0.97	139	6.35	2.4	5.43
D5	1.00	119	6.10	1.47	4.24
D6	0.92	122	6.48	1.59	4.49
MM	0.54	230	9.69	2.58	6.62
MDM	1.10	141	5.87	2.14	5.39

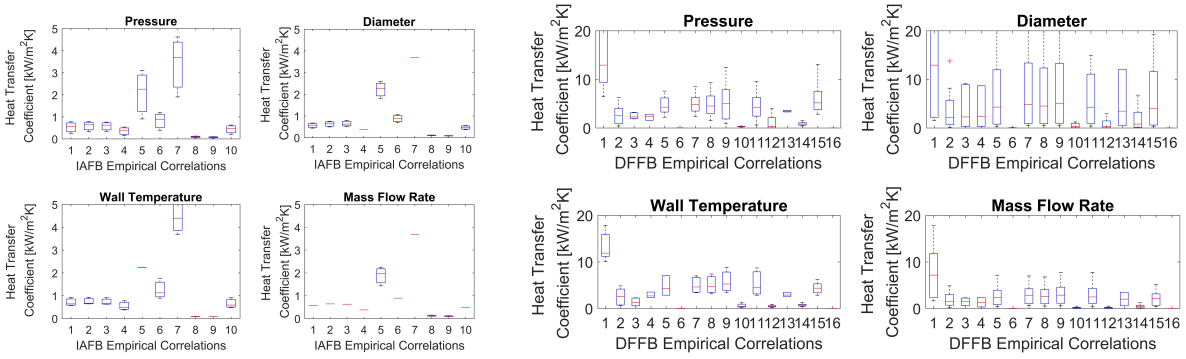

Figure 3: Sensitivity analysis results presented as a boxplot for the (a) IAFB and (b) DFFB regime.

Figure 4a shows the optimal Pareto fronts for Toluene, MM, MDM, D4, D5, and D6. The results illustrate that all the fluids experience similar trends. The volume and mass breakdown for the working fluids on the Pareto front (Figure 4a) that require the smallest volume are provided in Figure 5. The stored concentrator, receiver, and condenser are the three largest components for all the working fluids. These components, together with the regenerator, make up the heaviest components of the system. The receiver mass and volume become more dominant as the discharge time increases (lower inverse time values). For discharge times greater than 150 minutes (inverse time less than 0.2) there is a steep increase in volume. Toluene is shown to be the optimal working fluid for reducing the size of the system and increasing the discharge time and requires a minimum volume fraction of 20%. This is due to its higher thermal

efficiency. However, this advantage is at the expense of faster rotor rotational speeds and smaller rotor blade heights, refer to Table 4. The mass of the micro-ORC system is also important to investigate to ensure the launch vehicle constraints are met. Figure 5b, demonstrates that the mass fractions are approximately 8% higher than the volume fractions for low discharge times. At the highest discharge time, the volume fraction is nearly double the mass fraction due to the increase in PCM and insulation geometry. This highlights that volume is a more appropriate optimization variable than mass for this system.

Table 4 illustrates that the system using the toluene working fluid has a total specific power of 3.6 W/kg, which does not compete with solar photovoltaic systems. For example, the SMART-1 mission has an end of life specific density of 24 W/kg (mass includes the solar panels, the Power Control and Distribution Unit and Battery Management Electronics systems). When coupling the micro-ORC system to an STP system the shared specific power is improved to 8.7 W/kg assuming that the mass of the concentrator and receiver are part of the propulsion system (shared specific power excludes the receiver and concentrator mass but includes the margin). Despite the low specific power, the advantage to this system comes with the high-temperature thermal energy storage as it provides around 500 Wh/kg of specific energy that could be beneficial in future missions. By using boron instead of silicon, the specific energy could be increased up to 1280 Wh/kg. More efficient and lightweight concentrators, condensers, regenerators, and generators could increase the power density of the system. It was also found that inflatable concentrators are necessary for the feasibility of micro-ORC systems as deployable rigid concentrators (25% of rigid system) significantly exceed the spacecraft volume for the input power requirement, Figure 4b.

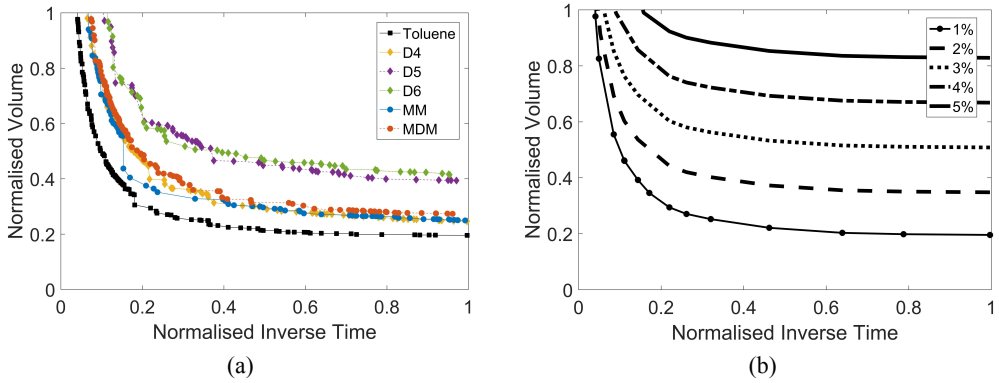

Figure 4: Pareto fronts of: (a) all the working fluids and (b) toluene with various concentrator sotrage volume percentages.

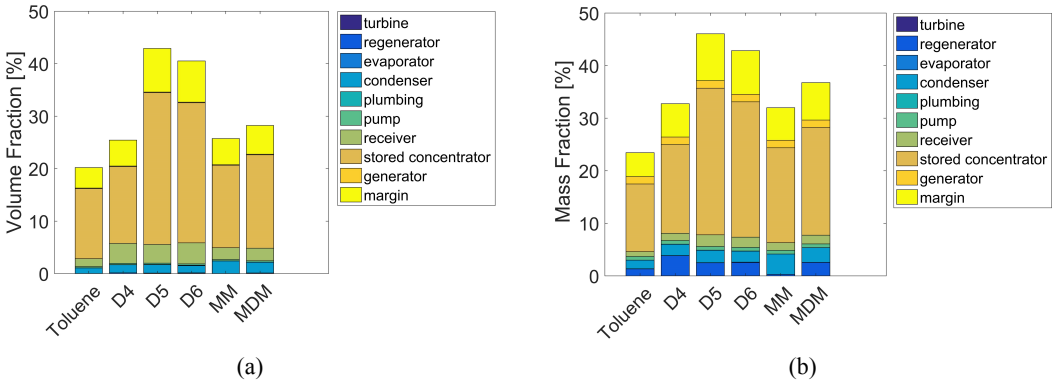

Figure 5: Breakdown charts of the (a) volume and (b) mass of the minimum volume result of the Pareto front (Figure 4a).

5. CONCLUSIONS

The study focused on the feasibility of micro-ORC systems for power generation on-board small satellites that use waste energy from a solar thermal propulsion system. A multi-objective optimization was performed on six working fluids, accounting for system design, satellite mission, and fluid constraints. From the resulting Pareto fronts, it has been found that toluene is the optimal fluid in terms of minimising the volume and maximising the discharge time. However, the turbine rotor has a small blade height (0.27 mm) and fast rotational speed (762 krpm), which which makes the attainment of high turbine efficiency challenging. The receiver and concentrator are the largest and heaviest components depending on the required discharge time. It was also found that the critical heat flux is necessary to determine the flow regime inside the evaporator when high-temperature phase change materials are used to better predict the heat transfer and therefore accurately determine the length and volume of the evaporator. However, the heat transfer coefficient of the evaporator has a negligible effect on the ORC volume. Various post CHF empirical equations were evaluated, and the Bromley and the Bishop correlations were found to provide the closest results to experimental data and mid-range results during the sensitivity analysis. Recommended future work is to conduct experimental testing and in-depth modelling of the evaporator-receiver coupling to predict the heat transfer better and characterize the off-design and transient effects of the system. The results indicate that micro-ORC systems are feasible on-board small satellites in terms of size and energy storage, and are attractive to missions requiring high specific energies, but they have low specific powers on the order of 8 W/kg when coupled to a solar thermal propulsion system.

REFERENCES

Angelino, G. and Invernizzi, C. (1993). Cyclic methylsiloxanes as working fluids for space power cycles. *J. of solar energy Eng.*, 115(3):130–137.

Angelino, G., Invernizzi, C., and Macchi, E. (1991). Organic working fluid optimization for space power cycles. In *Modern research topics in aerospace propulsion*, pages 297–326. Springer.

Antonio, M. D., Shi, C., Wu, B., and Khaligh, A. (2019). Design and Optimization of a Solar Power Conversion System for Space Applications. *IEEE Transactions on Industry Applications*.

Bahamonde, S., Pini, M., De Servi, C., Rubino, A., and Colonna, P. (2017). Method for the Preliminary Fluid Dynamic Design of High-Temperature Mini-Organic Rankine Cycle Turbines. *J. of Eng. for Gas Turbines & Power*, 139(8):82606.

Becker, K. M., Ling, C. H., Hedberg, S., and Strand, G. (1983). An experimental investigation of post dryout heat transfer. Technical report, Royal Inst. of Tech.

Bergman, T. L., Incropera, F. P., DeWitt, D. P., and Lavine, A. S. (2011). *Fundamentals of heat and mass transfer*. John Wiley & Sons, 7th edition.

Caputo, A. C., Pelagagge, P. M., and Salini, P. (2011). Joint economic optimization of heat exchanger design and maintenance policy. *Applied Thermal Eng.*, 31(8-9):1381–1392.

Colonna, P., Nannan, N. R., Guardone, A., and Lemmon, E. W. (2006). Multiparameter equations of state for selected siloxanes. *Fluid Phase Equilibria*, 244(2):193–211.

Colonna, P. and Van der Stelt, T. P. (2004). FluidProp: a program for the estimation of thermo physical properties of fluids. *Delft University of Technology, Delft, The Netherlands*.

Fréchette, L. G., Lee, C., and Arslan, S. (2004). Development of a mems-based rankine cycle steam turbine for power generation: project status. *Proc. PowerMEMS*, 4:28–30.

Gilmore, D. (2002). *Spacecraft thermal control handbook, Volume I: fundamental technologies*. American Institute of Aeronautics and Astronautics, Inc.

Gilpin, M. (2015). *High Temperature Latent Heat Thermal Energy Storage to augment Solar Thermal Propulsion for Microsatellites*. PhD thesis, University of Southern California.

Harinck, J., Colonna, P., Guardone, A., and Rebay, S. (2010). Influence of thermodynamic models in two-dimensional flow simulations of turboexpanders. *J. of turbomachinery*, 132(1):11001.

Henshall, P. (2006). A Proposal to Develop and Test a Fibre-Optic Coupled Solar Thermal Propulsion System for Microsatellites. Technical Report 0704-0188, Surrey University Guildford, UK.

Hewitt, G. F., Delhaye, J.-M., and Zuber, N. (2013). *Multiphase science and technology*, volume 2. Springer Science & Business Media.

Kim, S.-M. and Mudawar, I. (2013a). Universal approach to predicting heat transfer coefficient for condensing mini/micro-channel flow. *Int. J. of Heat & Mass Transfer*, 56(1-2):238–250.

Kim, S.-M. and Mudawar, I. (2013b). Universal approach to predicting saturated flow boiling heat transfer in mini/micro-channels– Part I. *Int. J. of Heat & Mass Transfer*, 64:1226–1238.

Kim, S.-M. and Mudawar, I. (2013c). Universal approach to predicting saturated flow boiling heat transfer in mini/micro-channels– Part II. *Int. J. of Heat & Mass Transfer*, 64:1239–1256.

Kreider, J. (1979). *Medium and High Temperature Solar Processes*. Energy Science and Engineering; Academic Press, Inc., New York.

Leverone, F., Cervone, A., and Gill, E. (2019). Cost analysis of solar thermal propulsion systems for microsatellite applications. *Acta Astronautica*, 155:90–110.

Leverone, F., Cervone, A., Pini, M., Gill, E., and Colonna, P. (2017). Feasibility of an Integrated Solar Thermal Power and Propulsion System for Small Satellites. In *68th IAC*, Adelaide.

Liamini, M., Shahriar, H., Vengallatore, S., and Fréchette, L. G. (2010). Design methodology for a rankine microturbine: Thermomechanical analysis and material selection. *J. of Microelectromechanical systems*, 20(1):339–351.

Montgomery, K., Buckner, J., Levin, Z., Cromer, J., and Wilt, D. (2019). Advanced Space Power Technology Development at the Air Force Research Laboratory. In *AIAA Scitech 2019 Forum*, page 1671.

Nakla, M. E., Groeneveld, D. C., and Cheng, S. C. (2011). Experimental study of inverted annular film boiling in a vertical tube cooled by R-134a. *Int. J. of Multiphase Flow*, 37(1):67–75.

Nguyen, N. H. and Moon, S.-K. (2015). An improved heat transfer correlation for developing post-dryout region in vertical tubes. *Nuclear Eng. & Technology*, 47(4):407–415.

Olla, P. (2009). *Space technologies for the benefit of human society and earth*. Springer, Dordrecht.

Orosz, M. (2009). Small scale solar ORC system for distributed power in Lesotho. In *Johannesburg, South Africa: Solar World Congress*.

Preißinger, M. and Brüggemann, D. (2016). Thermal stability of hexamethyldisiloxane (MM) for high-temperature organic Rankine cycle (ORC). *Energies*, 9(3):183.

Roudy, S. and Frechette, L. (2005). *Energy scavenging and nontraditional power sources for wireless sensor networks*. Wiley.

Schubert, D. (2012). Mems-concept using micro turbines for satellite power supply. In *Solar Power*. InTech.

Shah, M. M. (2017). Comprehensive correlation for dispersed flow film boiling heat transfer in mini/macro tubes. *Int. J. of Refrigeration*, 78:32–46.

Shah, Ramesh K and Sekulic, D. P. (2003). *Fundamentals of heat exchanger design*. John Wiley & Sons, Hoboken, NJ.

Surampudi, R., Blosiu, J., Bugga, R., Brandon, E., Smart, M., Elliott, J., Castillo, J., Yi, T., Lee, L., Piszczor, M., Miller, T., Reid, C., Taylor, C., Liu, S., Plichta, E., and Iannello, C. (2017a). Energy Storage Technologies for Future Planetary Science Missions. Technical report, NASA, USA.

Surampudi, R., Blosiu, J., Stella, P., Elliott, J., Castillo, J., Yi, T., Lyons, J., Piszczor, M., McNatt, J., Taylor, C., Gaddy, E., Liu, S., Plichta, E., and Iannello, C. (2017b). Solar Power Technologies for Future Planetary Science Missions. Technical report, NASA, USA.

Trimm, D. L., Akashah, S., Bishara, A., and Absi-Halabi, M. (1990). *Catalysts in Petroleum Refining 1989*. Studies in Surface Science and Catalysis. Elsevier Science.

Uusitalo, A., Turunen-Saaresti, T., Guardone, A., and Grönman, A. (2014). Design and flow analysis of a supersonic small scale ORC turbine stator with high molecular complexity working fluid. In *ASME Turbo Expo 2014: Turbine Technical Conference and Exposition*. ASME.

ACKNOWLEDGEMENT

The authors would like to thank Prof. Manfredo Gherardo Guilizzoni and Dr. Andrea Spinelli for their fruitful discussion on two-phase flow and organic fluids.